Effect of Piston Friction on the Performance of SI Engine: A New Thermodynamic Approach

E. Abu-Nada

I. Al-Hinti

A. Al-Sarkhi

B. Akash

Department of Mechanical Engineering,
Hashemite University,
Zarqa 13115, Jordan

This paper presents thermodynamic analysis of piston friction in spark-ignition internal combustion engines. The general effect of piston friction on engine performance was examined during cold starting and normal working conditions. Considerations were made using temperature-dependent specific heat model in order to make the analysis more realistic. A parametric study was performed covering wide range of dependent variables such as engine speed, taking into consideration piston friction combined with the variation of the specific heat with temperature, and heat loss from the cylinder. The results are presented for skirt friction only, and then for total piston friction (skirt and rings). The effect of oil viscosity is investigated over a wide range of engine speeds and oil temperatures. In general, it is found that oils with higher viscosities result in lower efficiency values. Using high viscosity oil can reduce the efficiency by more than 50% at cold oil temperatures. The efficiency maps for SAE 10, SAE 30, and SAE 50 are reported. The results of this model can be practically utilized to obtain optimized efficiency results either by selecting the optimum operating speed for a given oil type (viscosity) and temperature or by selecting the optimum oil type for a given operating speed and temperature. The effect of different piston ring configurations on the efficiency is also presented. Finally, the oil film thickness on the engine performance is studied in this paper. [DOI: 10.1115/1.2795777]

Introduction

In most previous studies on air-standard power cycles, friction is generally neglected for simplicity of the analysis [1–4]. However, due to the high revolution speed of the engine, this assumption becomes less realistic where a large percentage of engine power is dissipated into friction. Although air-standard power cycle analysis gives only approximation to the actual conditions and outputs [5], it would be very useful to study the cycle by including the effect of friction.

It is well known that reduction of engine mechanical friction increases the engine efficiency. Previous studies modeled the behavior of Otto, Diesel, and dual cycles including friction [6–8]. However, they dealt with average values of piston coefficient of friction and neglected type of lubricants and engine configuration details such as engine skirt and rings. Also, the dependence of friction on oil temperature was neglected in these studies. On the other hand, some studies have correlated the friction encountered in engines using empirical formulas [9,10]. In fact, these formulas are written in terms of engine speed and such correlations neglected engine operational details such as oil type, skirt, and ring configurations.

It is a fact that a large percentage of the mechanical friction loss in engines occur on the lubricated surfaces between the skirt and the cylinder liner as well as between the cylinder rings and cylinder liner [11]. The lubrication between rings and cylinder liner is effected by oil viscosity, oil film thickness, piston ring configuration, and the operational specifications of the engine. Besides, the friction between the piston skirt and the cylinder liner is affected by the clearance, piston tilt, piston skirt design, and surface roughness [12]. By considering energy consumption within the engine, it is found that friction loss contributes the major portion of the energy consumption developed in an engine. About two-thirds of it is caused by piston skirt friction, piston rings, and bearings, and the other third is due to the valve train, crankshaft, transmission, and gears [13]. Similar figures were reported by Kim et al. [14], who were successful in reducing engine friction through liner rotation. Piston ring lubrication models were used for prediction of engine cylinder friction. An accurate representation of lubrication conditions at the piston ring-cylinder liner interface is required for the estimation of frictional losses. Examples of the work conducted on modeling and analysis of the frictional losses at the piston ring-cylinder liner contact are given in Refs. [15–27]. Moreover, Xu et al. [28] presented two theoretical models that predict friction for piston ring and cylinder liner. Their work was compared to experimental findings. Also, Xu et al. proposed an inter-ring gas flow model by considering the effect of orifice flow through the ring end gap and ring side clearance [29].

It was found that piston ring friction force was higher than previously predicted. Also, it was pointed that fuel economy improvements exceeding 4% may result from combined application of reducing lubricant viscosity and proper surface treatment [30]. Their work was based on numerical findings using four different simulation methodologies, such as RINGPAK. Other studies have used RINGPAK tool in their engine friction simulation [31,32]. Other models are also available in literature [33,34].

The effect of viscosity on the oil film thickness and on the total friction force is significant. The oil viscosity is temperature dependent and under different engine conditions during cold start, normal operation, or severe operation condition, the viscosity of the lubricating oil changes significantly. A model for the prediction of the engine friction, including the viscosity effects, has been presented by Taylor [35]. The results include simulations for fully warmed-up and cold-start conditions, where the total engine friction is investigated. Accordingly, the total engine friction immediately after a cold start is about five times higher than the warmed-up conditions [35]. Further studies have been made on the oil film thickness of piston rings and effect of load and speed on oil film thickness [36]. Recently, more research has focused on the effect of oil film temperature on its thickness of piston rings [37–40]. Their results indicated that the oil film thickness could be

Submitted to ASME for publication in the JOURNAL OF ENGINEERING FOR GAS TURBINES AND POWER. Manuscript received July 19, 2006; final manuscript received August 27, 2007; published online January 22, 2008. Review conducted by Thomas W. Ryan III. Category: Internal Combustion Engines.

Copyright © 2008 by ASME

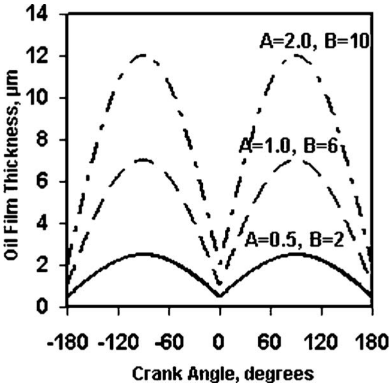

Fig. 1 Different distribution models for the ring oil film thickness

calculated by using the viscosity estimated from the oil film temperature [38]. It was reported that oil film thickness between the ring and liner increases with increasing oil viscosity [39]. Therefore, it can be seen that the temperature dependence of viscosity, engine operational conditions, and ring configuration are very essential in analyzing friction encountered in piston skirt and piston rings.

In the present work, a spark-ignition (SI) engine is analyzed by including the effect of skirt and ring friction on its performance. Different ring configurations and oil types are examined. Furthermore, the effect of oil film temperature on the skirt and ring friction is investigated. Moreover, this study evaluates the contribution of piston rings and skirt on the overall efficiency of the cycle and on the overall friction mean effective pressure (fmep). In addition, a temperature-dependent specific heat is considered.

Thermodynamic Analysis

Piston Friction. The piston friction work, in the combustion chamber, consists of two major parts, which are the skirt friction and pressure ring friction. By using Newton's law of viscosity, friction work is defined as

$$\delta W_{\text{irrev}} = \left(\mu \frac{du}{dy}\right)_{\text{skirt}} L_{\text{skirt}} \pi D \Delta x + \left(\mu \frac{du}{dy}\right)_{\text{ring}} L_{\text{ring}} \pi D \Delta x \qquad (1)$$

The friction work (irreversible work) can be expressed in terms of instantaneous piston speed as

$$\delta W_{\text{irrev}} = \mu \frac{U_p(\theta)}{C} L_{\text{skirt}} \pi D \Delta x + \mu \frac{U_p(\theta)}{\varepsilon} L_{\text{ring}} \pi D \Delta x \qquad (2)$$

where C is the skirt clearance and ε is the clearance between the liner and the pressure ring. In the present study, the value of C is taken as a constant to represent the average clearance between the cylinder liner and the skirt of the piston. However, ε is taken as the oil film thickness between the ring and cylinder liner. This thickness reaches a minimum value at the bottom dead center (BDC) and top dead center (TDC) and has higher values between them [36,38]. The distribution of oil film thickness with crank angle was reported [38,41]. The shape of the oil film thickness can be approximated by a trigonometric function where minimum values at BDC and TDC and higher values in between. In the current study, the following distribution is assumed that agrees with the trend of previous published work:

$$\varepsilon(\theta) = A + B|\sin(\theta)| \qquad (3)$$

where A and B are constants. Figure 1 gives a representation of three different distributions of ring oil film thickness obtained by using different combinations of A and B. These values are chosen to agree with distributions reported in literature [36,38,41].

The instantaneous piston speed, in Eq. (2), can be expressed in terms of average piston speed as [11]

$$U_p(\theta) = \overline{U_p}\frac{\pi}{2}\sin(\theta)\left(1 + \frac{\cos(\theta)}{\left(\left(\frac{\ell}{R}\right) - \sin^2(\theta)\right)^{1/2}}\right) \qquad (4)$$

Thus, the friction work in Eq. (2) is written as

$$\delta W_{\text{irrev}} = \mu \pi D \Delta x \overline{U_p}\frac{\pi}{2}\sin(\theta)\left(1 + \frac{\cos(\theta)}{\left(\left(\frac{\ell}{R}\right) - \sin^2(\theta)\right)^{1/2}}\right) \times \left(\frac{L_{\text{skirt}}}{C} + \frac{L_{\text{ring}}}{\varepsilon}\right) \qquad (5)$$

Thermodynamic properties of air. In most air-standard power cycle models, air is assumed to behave as an ideal gas with constant specific heats. The values of specific heats are usually used as cold properties. However, this assumption can be valid only for small temperature differences. Therefore, the assumption would produce greater error in all air-standard power cycles. In order to account for the large temperature difference encountered in air-standard power cycles, constant average values of specific heats and specific heat ratios are sometimes used. These average values are evaluated using the extreme temperatures of the cycle, and are believed to yield better results. Obviously, this remains a rough simplification and can result in significant deviations from reality. Thus, the incorporation of variable specific heats in air-standard power cycle models can improve their predictions and bring them closer to reality.

An equation that can be used, for the temperature range 300–3500 K, is obtained from Sonntag et al. [42]. It is based on the assumption that air is an ideal gas mixture containing 78.1% nitrogen, 20.95% oxygen, 0.92% argon, and 0.03% carbon dioxide (on mole basis). It is presented in the following equation:

$$\begin{aligned} C_p = {} & 2.506 \times 10^{-11} T_g^2 + 1.454 \times 10^{-7} T_g^{1.5} - 4.246 \times 10^{-7} T_g \\ & + 3.162 \times 10^{-5} T_g^{0.5} + 1.3303 - 1.512 \times 10^{4} T_g^{-1.5} \\ & + 3.063 \times 10^{5} T_g^{-2} - 2.212 \times 10^{7} T_g^{-3} \end{aligned} \qquad (6)$$

The results obtained from the above equation are in agreement with those reported in literature [43]. It is found from Eq. (6) that specific heat at constant pressure increases with temperature from about 1.0 kJ/kg K at 300 K to about 1.3 kJ/kg K at about 3000 K. Surely, such difference should be taken into consideration. Similarly, the specific heat ratio k decreases from 1.40 to about 1.28 within the same temperature range.

Thermodynamic analysis. For a closed system and a small change of the process, the first law of thermodynamics is simply written as

$$\delta Q - \delta W = dU \qquad (7)$$

Therefore, by using the definition of work, the first law can be expressed as

$$\delta Q_{\text{in}} - \delta Q_{\text{loss}} - (PdV - \delta W_{\text{irrev}}) = dU \qquad (8)$$

where the irreversible work is mainly due to friction work.

For an ideal gas, the equation of state is expressed as

$$PV = mR_g T_g \qquad (9)$$

By differentiating Eq. (9), we can get

$$PdV + VdP = mR_g dT_g \qquad (10)$$

Also, for an ideal gas with constant specific heats, the change in internal energy is expressed as

$$dU = mC_v dT_g \qquad (11)$$

By substituting Eq. (11) into Eq. (10), then

$$dU = \frac{C_v}{R_g}(PdV + VdP) \quad (12)$$

By substituting Eq. (12) into Eq. (8), the following equation is obtained:

$$\delta Q_{\text{in}} - \delta Q_{\text{loss}} - (PdV - \delta W_{\text{irrev}}) = \frac{C_v}{R_g}(PdV + VdP) \quad (13)$$

where the δW_{irrev} is given by Eq. (5). The total amount of heat input to the cylinder by combustion of fuel in one cycle is

$$\delta Q_{\text{in}} = m_f \text{LHV} \quad (14)$$

The total heat added from the fuel to the system until the crank position reaches angle θ is given as

$$\delta Q(\theta) = \delta Q_{\text{in}} x_b \quad (15)$$

where x_b is the Weibe function that is used to determine the combustion rate of the fuel and is expressed as [11]

$$x_b = 1 - \exp\left(-a\left(\frac{\theta - \theta_s}{\Delta\theta}\right)^n\right) \quad (16)$$

where a and n equal to 5 and 3, respectively. Also, the total amount of heat loss from the system when the crank moves an increment of $d\theta$ is given as

$$\delta Q_{\text{loss}} = \frac{h_{\text{cg}} A_h}{\omega}(T_g - T_w)d\theta \quad (17)$$

By substituting Eqs. (14)–(17) into Eq. (13) followed by differentiation with respect to crank angle (θ), the following equation is obtained:

$$\frac{dP}{d\theta} = \frac{k-1}{V}\left(\delta Q_{\text{in}}\frac{dx_b}{d\theta} - \frac{h_{\text{cg}}A_h}{\omega}(T_g - T_w)\frac{\pi}{180}\right) - k\frac{P}{V}\frac{dV}{d\theta} + \frac{k-1}{V}(\delta W_{\text{irrev}})\frac{dx}{d\theta} \quad (18)$$

Equation (18) can be solved by using explicit finite difference technique with second order accurate differentiation. The result is given as

$$\begin{aligned} P(\theta) &= \frac{4}{3}P(\theta - \Delta\theta) - \frac{1}{3}P(\theta - 2\Delta\theta) + \frac{k-1}{3V}\delta Q_{\text{in}}(3x_b(\theta) \\ &\quad - 4x_b(\theta - \Delta\theta) + x_b(\theta - 2\Delta\theta)) + \frac{2}{3}\frac{(k-1)}{3V} \\ &\quad \times (h_{\text{cg}}A_h(\theta)(T_g - T_w))\frac{1}{\omega} - \frac{2kP(\theta - \Delta\theta)}{3V(\theta)} \\ &\quad \times \left(\frac{V(\theta + \Delta\theta) - V(\theta + \Delta\theta)}{2\Delta\theta}\right) + \frac{2}{3}\frac{(k-1)}{3V}\delta W_{\text{irev}}\frac{dx}{d\theta}\Delta\theta \end{aligned} \quad (19)$$

where $dP/d\theta$ is expressed as

$$\frac{dP}{d\theta} = \frac{3P(\theta) - 4P(\theta - \Delta\theta) + P(\theta - 2\Delta\theta)}{2\Delta\theta} \quad (20)$$

The instantaneous cylinder volume, area, and displacement are given by the slider crank model as [11]

$$V(\theta) = V_c + \frac{\pi D^2}{4}x(\theta) \quad (21)$$

$$A_h(\theta) = \frac{\pi D^2}{4} + \frac{\pi DS}{2}(R + 1 - \cos(\theta) + (R^2 - \sin^2(\theta))^{1/2}) \quad (22)$$

Table 1 Engine and operational specifications used in simulation

Fuel	C_8H_{18}
Compression ratio	8.3
Cylinder bore (m)	0.0864
Stroke (m)	0.0674
Skirt length (m)	0.0674
Skirt clearance (m)	2.3×10^{-5}
Connecting rod length (m)	0.13
Crank radius (m)	0.0337
Clearance volume (m^3)	5.41×10^{-5}
Swept volume (m^3)	3.95×10^{-4}
Inlet pressure (bar)	1
Inlet temperature (K)	300
Equivalence ratio	1
Ignition timing	−25 deg BTDC
Duration of combustion	70 deg
Wall temperature (K)	400

$$x(\theta) = (\ell + R) - (R\cos(\theta) + (\ell^2 - \sin^2(\theta))^{1/2}) \quad (23)$$

Once the pressure is calculated, the temperature of the gases in the cylinder can be calculated using the equation of state as

$$T_g = \frac{P(\theta)V(\theta)}{mR_g} \quad (24)$$

The convective heat transfer coefficient in Eq. (17) h_{cg} is given by the Woschni model as [44–46]

$$h_{\text{cg}} = 3.26D^{-0.2}P^{0.8}T_g^{-0.55}w^{0.8} \quad (25)$$

where w is the velocity of the burned gas and is given as

$$w(\theta) = \left(C_1\overline{U_p} + C_2\frac{V_d T_{\text{gr}}}{P_r V_r}(P(\theta) - P_m)\right) \quad (26)$$

In the above equation, the displacement volume is V_d. However, V_r, T_{gr}, and P_r are reference state properties at closing of inlet valve and P_m is the pressure at the same position to obtain P without combustion (pressure values in cranking). The values of C_1 and C_2 are given as follows: For compression, C_1=2.28, C_2=0 and for combustion and expansion, C_1=2.28, C_2=0.00324.

Solution Methodology

Equation (19) is solved for each crank angle for $-180 \leq \theta \leq 180$ using a step size $\Delta\theta$=1 deg. The values of $\theta = \pm 180$ correspond to BDC whereas the value of θ=0 corresponds to TDC. The heat addition in Eq. (19) is only valid for $\theta_s < \theta < (\theta_s + \Delta\theta)$, i.e., during the period of combustion. In solving Eq. (19), notice that k, P, T, and h_{cg} are coupled, i.e., solution of one of these variables depends on the solution of others. The solution procedure is as follows: By knowing the pressure of the gases at the BDC, the initial temperature of the gases is first calculated using Eq. (24). Then, the value of the pressure, after an increment of $\Delta\theta$, is determined using Eq. (18). Once the value of the pressure is obtained, the temperature-dependent properties $C_p(T)$ is calculated by using Eq. (6). The value of $C_v(T)$ is then determined from the relation $[C_v(T) = C_p(T) - R]$. Thereafter, the value of k is calculated as $k(T) = C_p(T)/C_v(T)$. Finally, the heat transfer coefficient is calculated using the Woschni model given by Eq. (25). The above mentioned procedure is repeated for each value of θ many times until the change between two successive iterations for all variables (T, P, k, and h_{cg}) is less than 10^{-4}. After solving for the pressure in the cylinder, the total friction work for skirt and rings was calculated by integrating Eq. (5) for $-180 \text{ deg} \leq \theta \leq 180$ deg. Then, the fmep is calculated as

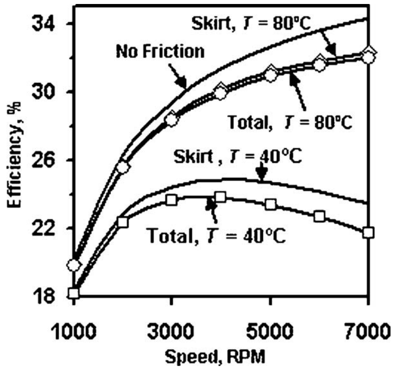

Fig. 2 Efficiency versus engine speed for skirt and total friction contribution, SAE 30, A=1, B=6, number of rings=2 (each 1.5 mm thick), C=23 μm

$$\text{fmep} = \frac{W_{\text{friction}}}{V_d} \tag{27}$$

The indicated work is calculated by integrating the PV diagram as

$$W_i = \int_{\theta=-180}^{\theta=180} pdV \tag{28}$$

The brake work is calculated as

$$W_b = W_i - W_f \tag{29}$$

Finally, the thermal efficiency is calculated as

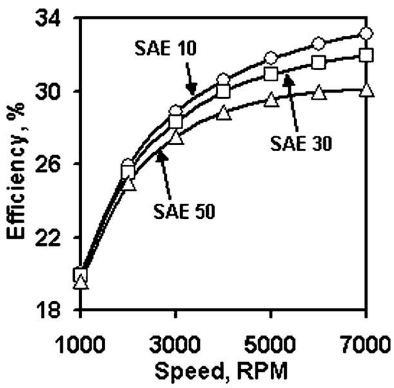

(a)

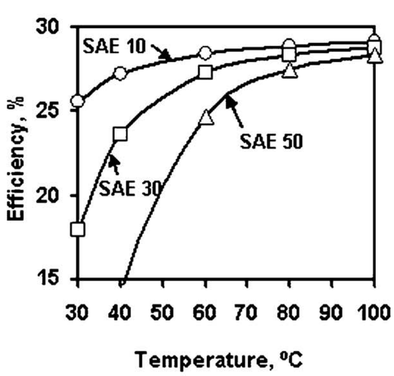

(b)

Fig. 3 (a) Efficiency versus engine speed for various oil types at 80°C, (b) Efficiency versus oil temperature for various oil types at 3000 rpm. (Both (a) and (b) have A=1, B=6, number of rings=2 (each 1.5 mm thick), C=23 μm.)

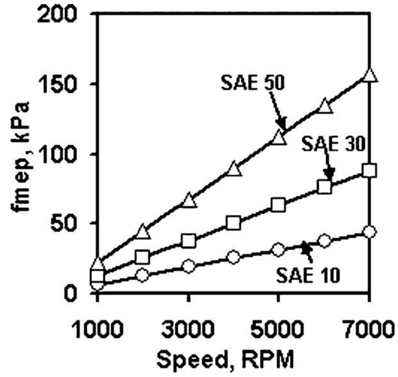

(a)

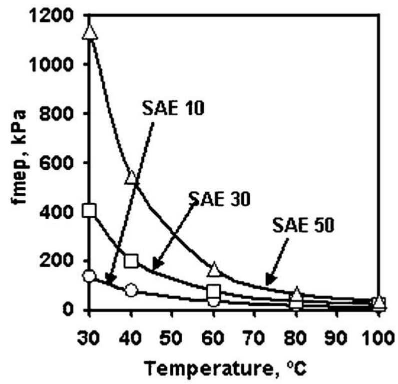

(b)

Fig. 4 (a) fmep versus engine speed for various oil types at 80°C, (b) fmep versus oil temperature for various oil types and 3000 rpm. (Both (a) and (b) have A=1, B=6, number of rings =2 (each 1.5 mm thick), C=23 μm.)

$$\eta_{\text{th}} = \frac{W_b}{m_f \text{LHV}} \tag{30}$$

A parametric study has been performed based on the numerical solution of Eq. (19). The study covers wide range of dependent variables such as engine speed, taking into consideration piston friction combined with the variation of temperature-dependent specific heat, and heat loss from the cylinder. Engine specifications, dimensions, and other constants used in the parametric study are listed in Table 1.

Results and Discussion

In order to examine the general effect of piston friction on engine performance, Fig. 2 is presented. It shows engine's thermal efficiency with two oil temperatures: 40°C and 80°C; one representing cold-start conditions, while the other representing normal operating conditions. For each condition, two cases were considered; first, considering skirt friction only, and second considering total piston friction (i.e., skirt and rings). They were compared to frictionless piston, which is usually assumed in most thermodynamic analyses that do not consider piston friction. An observation can be drawn from this figure in which the inclusion of the piston friction in efficiency evaluation can reduce the calculated values. This becomes particularly significant in the high speed range and at low oil temperatures. Also, the minimal effect of ring friction in comparison to skirt friction is clearly illustrated. Although the contribution of ring friction becomes more significant at low oil temperatures and high engine speeds, skirt friction remains the dominant factor in piston friction.

The effect of oil viscosity is investigated in Fig. 3 over a wide

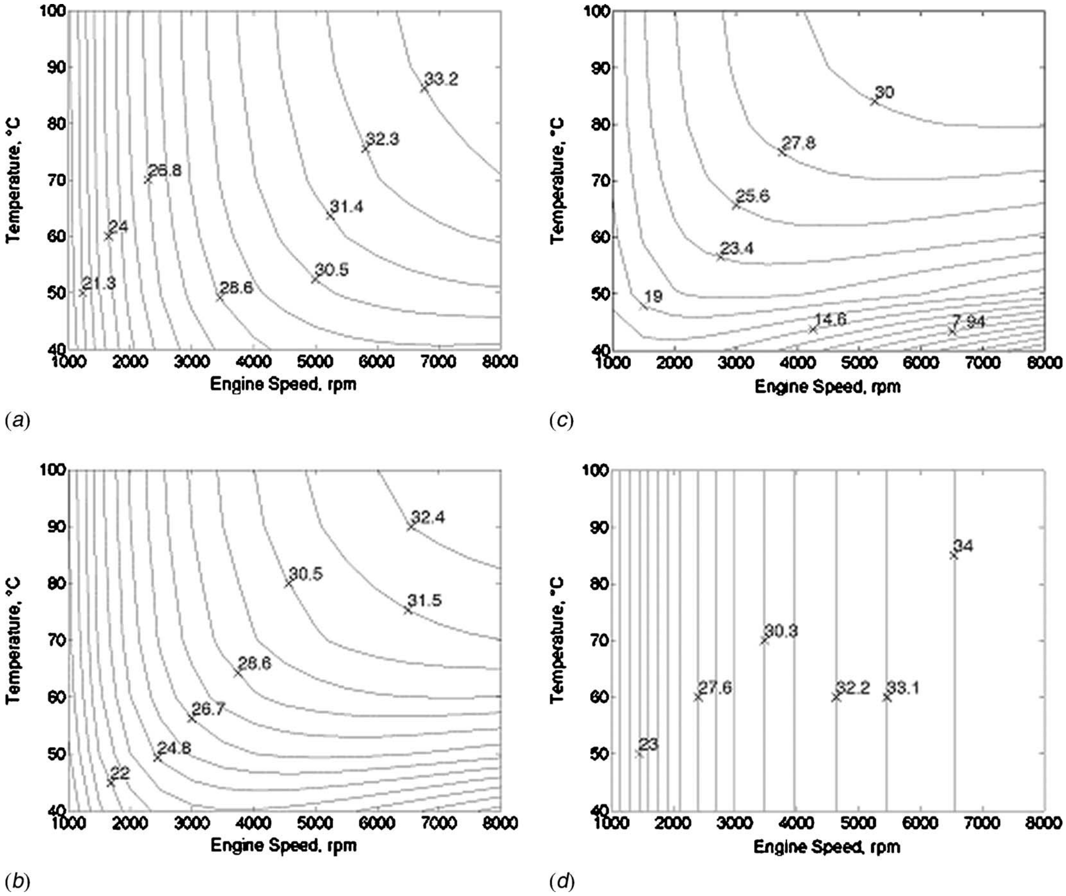

Fig. 5 Efficiency contours $A=1$, $B=6$, number of rings=2 (each 1.5 mm thick), $C=23$ μm: (*a*) SAE 10, (*b*) SAE 30, (*c*) SAE 50, and (*d*), no friction case

range of engine speeds and oil temperatures, as shown in parts (*a*) and (*b*), respectively. In general, oils with higher SAE numbers result in lower efficiency values due to their higher viscosities. Under normal operating conditions (i.e., relatively high oil temperatures), the difference in performance with the application of different oils is minimal at low speeds and only starts to become more pronounced at high speeds. However, as demonstrated in Fig. 3(*b*), this changes completely at lower oil temperatures, which could be encountered at cold starts. Using high viscosity oil can reduce the efficiency by over 50% at cold oil temperatures.

In order to analyze how the friction irreversible work is affected by the speed and the oil temperature, Fig. 4 is presented. As it can be seen from Fig. 4(*a*), the fmep increases linearly with engine speed. This trend is expected from the examination of Eq. (5) where the piston friction work is linearly related to the piston speed. However, Fig. 4(*b*) reveals a strong dependence of the fmep on the temperature. This is due to the strong dependence of the viscosity of lubricating oils on temperature over the range of temperatures, practically, encountered during engine operations. About 50°C drop in oil temperature can increase its viscosity by an order of magnitude.

The efficiency maps for SAE 10, SAE 30, and SAE 50 are given in Fig. 5. It illustrates how the results of this model can be practically utilized to obtain optimized efficiency results either by selecting the optimum operating speed for a given oil type (i.e., viscosity), temperature, and engine speed. For example, the efficiency at a given speed is less dependent on the oil temperature for SAE 10 oil as compared to SAE 50. Therefore, it is much easier to obtain high efficiency values at high speeds with low oil temperatures when SAE 10 is used in comparison with SAE 50. On the other hand, for a given oil (e.g., SAE 30), in order to achieve the efficiency obtained at a low-medium range speed with high oil temperatures, higher engine speeds are required with low oil temperatures. Figure 5(*d*) presents the resulting map without the inclusion of piston friction in the analysis. Similar maps could also be obtained when empirical formulas relating the engine friction to the engine speed are used [9,47]. Obviously, such map is rather theoretical and totally oblivious to the effect of oil type or temperature and thus it is of limited use in practical considerations.

Figure 6 demonstrates the effect of different piston ring configurations on the efficiency. As expected, increasing the number or thickness of piston rings increases piston friction and thus reduces the brake power and the efficiency. However, the effect of changing piston ring configuration is limited in comparison to other parameters. This is due to dominance of skirt friction over ring friction, which was illustrated in Fig. 2. As explained earlier and shown in Fig. 1, the oil film thickness between the ring and the cylinder liner varies with crank angle and can be approximated with the trigonometric function given in Eq. (3).

In order to examine the effect of oil film thickness on engine performance, Fig. 7 is presented. It shows the effect of speed and temperature on efficiency for three different values of constants A and B in Eq. (3) yielding three different oil film distributions. Although decreasing oil film thickness results in a drop in efficiency, this effect becomes noticeable only at low temperatures and at high engine speeds. It is also interesting to note that the two distributions assume maximum film thicknesses as of 7 μm and 12 μm resulted in nearly identical efficiency curves. However, the third distribution that assumes a maximum film thickness of 2.5 μm resulted in a somewhat different curve. This suggests that

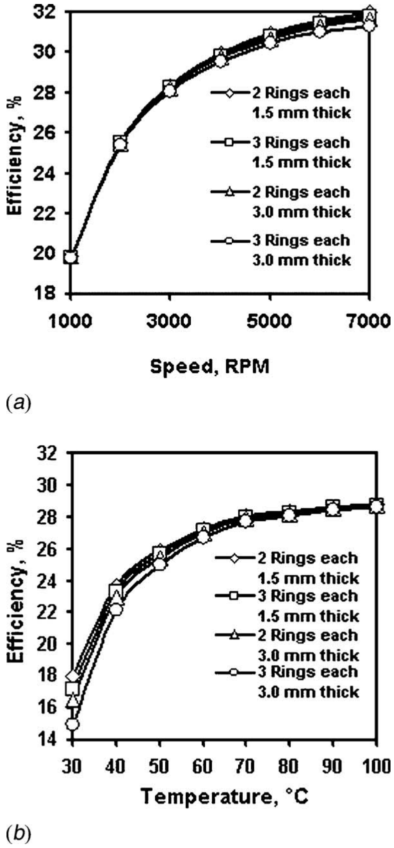

Fig. 6 (*a*) Efficiency versus engine speed for different ring configuration, SAE 30, $T=80°C$, $A=1$, $B=6$, $C=23\ \mu m$. (b) Efficiency versus oil temperature for different ring configuration for SAE 30, $N=3000°C$, $A=1$, $B=6$, $C=23\ \mu m$.

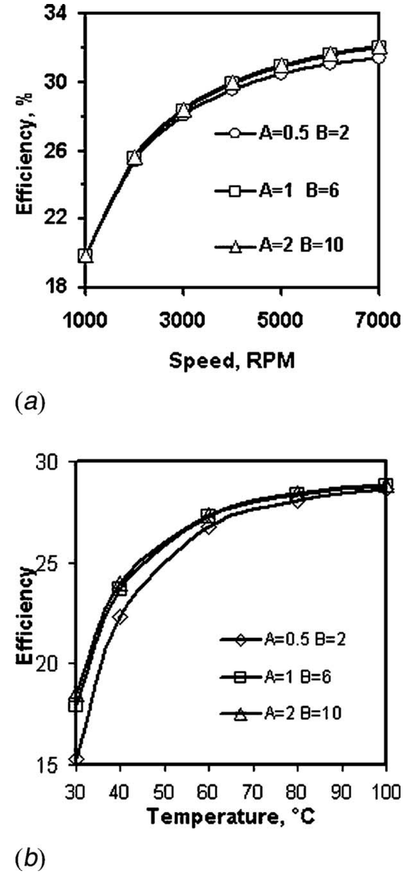

Fig. 7 (a) Efficiency versus engine speed for various oil film thickness, SAE 30, $T=80°C$, number of rings=2 (each 1.5 mm thick), $C=23\ \mu m$. (b) Efficiency versus oil temperature for various oil film thickness, SAE 30, $N=3000$, $A=1$, $B=6$, number of rings=2 (each 1.5 mm thick), $C=23\ \mu m$.

there exists a threshold value in the order of 1 μm for the oil film thickness, below which ring friction can start to play significant role in piston friction.

Conclusions

The performance of a SI engine has been analyzed by including the effect of skirt and ring frictions. Different ring configurations and oil types were examined. The effect of oil film temperature on the skirt and the ring friction has been investigated. A parametric study has been performed covering wide range of dependent variables such as engine speed, by considering piston friction combined with temperature-dependent specific heat, and heat loss from the cylinder. Moreover, this study has evaluated the contribution of piston skirt and rings on the overall cycle efficiency. Cases of cold-start and warm-up conditions were presented; first considering skirt friction only, and second with the consideration of total piston friction (skirt and rings). It was found that the inclusion of the piston friction in efficiency evaluation can reduce the calculated values especially in high speed range and at low oil temperatures. Although the contribution of ring friction becomes more significant at low oil temperatures and high engine speeds, skirt friction remains the dominant factor in piston friction.

The effect of oil viscosity over a wide range of engine speeds and oil temperatures implies that oils with higher viscosities result in lower efficiency values. Alternatively, under normal operation conditions, the difference in performance with the application of different oils is minimal at low speeds and only starts to become more pronounced at high speeds. However, using high viscosity oil can reduce the efficiency by more than 50% at cold oil temperatures. Also, the fmep increases linearly with engine speed. It has strong dependence on the temperature and viscosity. A drop in oil temperature by 50°C can result in an increase of its viscosity by an order of magnitude.

The efficiency maps for SAE 10, SAE 30, and SAE 50 are developed. They illustrate how the results of this model can be practically utilized in efficiency calculations. The oil film thickness between the ring and the cylinder liner varies with the position of the crank angle. Although it can be generally stated that decreasing the oil film thickness results in a drop in the efficiency, this effect becomes noticeable only at low temperatures and at high engine speeds. It is concluded that the two distributions that assume maximum film thicknesses of 7 μm and 12 μm resulted in nearly identical efficiency curves. However, the third distribution that assumes a maximum film thickness of 2.5 μm resulted in a somewhat different curve. This suggests that there exists a threshold value in the order of 1 μm for the oil film thickness, below which ring friction can start to play a significant role in piston friction.

Nomenclature

A_h = heat transfer area (m^2)
A = coefficient in oil film thickness equation (m)
a = constant in Weibe function
B = coefficient in oil film thickness equation (m)
C = skirt clearance (m)
C_p = constant pressure specific heat (kJ/kg K)
C_v = constant volume specific heat (kJ/kg K)
D = cylinder diameter (m)

h_{cg} = heat transfer coefficient for gases in the cylinder (W/m^2 K)
k = specific heat ratio, dimensionless
L_{ring} = ring thickness
L_{skirt} = skirt length
LHV = lower heating value (kJ/kg)
ℓ = connecting rod length (m)
m = mass of cylinder contents (kg)
m_f = mass of burned fuel (kg)
n = constant in Weibe function
P = pressure inside cylinder (Pa)
P_i = inlet pressure (Pa)
Q = heat transfer (kJ)
Q_{in} = heat added from burning fuel (kJ)
R = crank radius (m)
R_g = gas constant (kJ/kg K)
T = oil temperature in the cylinder (°C)
T_g = gas temperature in the cylinder (K)
T_i = inlet temperature (K)
T_w = cylinder temperature (K)
U = internal energy (kJ)
U_p = piston speed (m/s)
$\overline{U_p}$ = average piston speed (m/s)
V = cylinder volume (m^3)
V_c = clearance volume (m^3)
V_d = displacement volume (m^3)
x = distance from top dead center (m)
x_b = burning rate of the fuel, dimensionless
W_i = indicated work (J)
W_b = brake work (J)
$W_{friction}$ = friction work (J)
W_{irrev} = irreversible work (J)
w = average cylinder gas velocity (m/s)
α = thermal diffusivity (m^2/s)
ε = oil film thickness (m)
θ = angle (deg)
θ_s = start of combustion or heat addition (deg)
$\Delta\theta$ = duration of combustion (deg)
μ = oil dynamic viscosity ($N\,s/m^2$)
η_{th} = thermal efficiency (%)

Abbreviations

fmep = friction mean effective pressure (kPa)
bmep = brake mean effective pressure (kPa)
imep = indicated mean effective pressure (kPa)
irrev = irreversible
TDC = top dead center
BDC = bottom dead center

References

[1] Al-Sarkhi, A., Jaber, J., Abu-Qudais, M., and Probert, S., 2006, "Effects of Friction and Temperature-Dependent Specific-Heat of the Working Fluid on the Performance of a Diesel-Engine," Appl. Energy, **83**(2), pp. 153–165.
[2] Ge, Y., Chen, L., Sun, F., and Wu, C., 2005, "Thermodynamic Simulation of Performance of Otto Cycle With Heat Transfer and Variable Specific Heats of Working Fluid," Int. J. Therm. Sci., **44**(5), pp. 506–511.
[3] Jafari, A., and Hannani, S., 2006, "Effect of Fuel and Engine Operational Characteristics on the Heat Loss From Combustion Chamber Surfaces of SI Engines," Int. Commun. Heat Mass Transfer, **33**, pp. 122–124.
[4] Ozsoysal, O., 2006, "Heat Loss as a Percentage of Fuel's Energy in Air Standard Otto and Diesel Cycles," Energy Convers. Manage., **47**, pp. 1051–1062.
[5] Pulkrabek, W., 2004, *Engineering Fundamentals of the Internal Combustion Engine*, 2nd ed., Prentice-Hall, Englewood Cliffs, NJ.
[6] Angulo-Brown, F., Fernandez-Betanzos, J., and Diaz-Pico, C. A., 1994, "Compression Ratio of an Optimized Otto-Cycle Model," Eur. J. Phys., **15**(1), pp. 38–42.
[7] Chen, L., Lin, J., Luo, J., Sun, F., and Wu, C., 2002, "Friction Effects on the Characteristic Performance of Diesel Engines," Int. J. Energy Res., **26**(10), pp. 965–971.
[8] Wang, W., Chen, L., Sun, F., and Wu, C., 2002, "The Effects of Friction on the Performance of an Air Standard Dual Cycle," Exergy, **2**(4), pp. 340–344.
[9] Patton, K. J., Nitschke, R. G., and Heywood, J. B., 1989, "Development and Evaluation of a Friction Model for Spark Ignition Engine," SAE Paper No. 890836.
[10] Bishop, I. N., 1973, "Effect of Design Variables on Friction and Economy," SAE Paper No. 640807.
[11] Ferguson, C., and Kirkpatrick, A., 2001, *Internal Combustion Engines: Applied Thermosciences*, Wiley, New York.
[12] Röhrle, M. D., 1995, *Pistons for Internal Combustion Engines: Fundamentals of Piston Technology*, MAHLE GmbH, Verlag Moderne Industrie, Landsberg/Lech, Germany, p. 70.
[13] Tung, S. C., and McMillan, M. L., 2004, "Automotive Tribology Overview of Current Advances and Challenges for the Future," Tribol. Int., **37**, pp. 517–536.
[14] Kim, M., Dardalis, D., Matthews, R. D., and Kiehne, T. M., 2005, "Engine Friction Reduction Through Liner Rotation," SAE Paper No. 2005-01-1652.
[15] Rohde, S. M., Whitaker, K. W., and McAllister, G. T., 1980, "A Mixed Friction Model for Dynamically Loaded Contacts With Application to Piston Ring Lubrication, Surface Roughness Effects in Hydrodynamic and Mixed Lubrication," *ASME Winter Annual Meeting*, pp. 19–50.
[16] Dowson, D., Economou, P. N., Ruddy, B. L., Strachan, P. J., and Baker, A. J., 1979, "Piston Ring Lubrication, Part II-Theoretical Analysis of a Single Ring and a Complete Ring Pack, Energy Conservation Through Fluid Film Lubrication Technology, Frontiers in Research and Design," *ASME Winter Annual Meeting*, pp. 23–52.
[17] Aoyama, S., 1994, "Numerical Simulation of Piston Ring in Mixed Lubrication: A Non-Axisymmetrical Analysis," ASME J. Tribol., **116**, pp. 470–478.
[18] Yang, Q., and Keith, T. G., 1995, "An Elasto-Hydrodynamic Cavitation Algorithm for Piston Ring Lubrication," STLE Tribol. Trans., **38**, pp. 97–107.
[19] Sawicki, J., and Yu, B., 2000, "Analytical Solution of Piston Ring Lubrication Using Mass Conserving Cavitation Algorithm," STLE Tribol. Trans., **43**, pp. 587–594.
[20] Akalin, O., and Newaz, G. M., 2001, "Piston Ring-Cylinder Bore Friction Modeling in Mixed Lubrication Regime, Part I-Analytical Results," ASME J. Tribol., **123**, pp. 211–218.
[21] Akalin, O., and Newaz, G. M., 2001, "Piston Ring-Cylinder Bore Friction Modeling in Mixed Lubrication Regime: Part II-Correlation With Bench Test Data," ASME J. Tribol., **123**, pp. 219–223.
[22] Priest, M., Dowson, D., and Taylor, C. M., 2000, "Theoretical Modeling of Cavitation in Piston Ring Lubrication," Proc. Inst. Mech. Eng., Part C: J. Mech. Eng. Sci., **214**, pp. 435–447.
[23] Ting, L. L., 1993, "Development of a Reciprocating Test Rig for Tribological Studies of Piston Engine Moving Components: Part 1—Rig Design and Piston Ring Friction Coefficients Measuring Method," SAE Paper No. 930685.
[24] Ting, L. L., 1993, "Development of a Reciprocating Test Rig for Tribological Studies of Piston Engine Moving Components: Part 2—Measurements of Piston Ring Coefficients and Rig Test Confirmation," SAE Paper No. 930686.
[25] Dearlove, J., and Cheng, W. K., 1995, "Simultaneous Piston Ring Friction and Oil Film Thickness Measurements in a Reciprocating Test Rig," SAE Paper No. 952470.
[26] Arcoumanis, C., Duszynski, M., Flora, H., and Ostovar, P., 1995, "Development of a Piston-Ring Lubrication Test-Rig and Investigation of Boundary Conditions for Modeling Lubrication Film Properties," SAE Paper No. 952468.
[27] Bolander, N. W., Steenwyk, B. D., Kumar, A., and Sadeghi, F., 2004, "Film Thickness and Friction Measurement of Piston Ring Cylinder Liner Contact With Corresponding Modeling Including Mixed Lubrication," *ASME-ICED Fall Technical Conference Proceedings*, ASME Paper No. ICEF2004-903.
[28] Xu, H., Bryant, M. D., Matthews, R. D., Kiehne, T. M., Steenwyk, B. D., Bolander, N. W., and Sadeghi, F., 2004, "Friction Prediction for Piston Ring-Cylinder Liner Lubrication," *presented at the ASME Internal Combustion Engine Division Conference*, Long Beach, CA, Oct. 2004, ASME Paper No. ICEF2004-885; also in *Proceedings of the ASME Internal Combustion Engine Division: 2004 Fall Technical Conference*.
[29] Xu, H., Kim, M., Dardalis, D., Bryant, M. D., Matthews, R. D., and Kiehne, T. M., 2005, "Numerical and Experimental Investigation of Piston Ring Friction," *presented at the ASME Internal Combustion Engine Division Conference*, Chicago, IL, Apr. 5–7, ASME Paper No. ICES 2005-1086; also in *Proceedings of the ASME Internal Combustion Engine Division: 2005 Spring Technical Conference*.
[30] Fox, I. E., 2005, "Numerical Evaluation of the Potential for Fuel Economy Improvement Due to Boundary Friction Reduction Within Heavy-Duty Diesel Engines," Tribol. Int., **38**, pp. 265–275.
[31] Gulwadi, S. D., 1998, "A Mixed Lubrication and Oil Transport Model for Piston Rings Using a Mass Conservation Algorithm," ASME J. Eng. Gas Turbines Power, **120**, pp. 199–208.
[32] Piao, Y., and Gulwadi, S. D., 2003, "Numerical Investigation of the Effects of Axial Cylinder Bore Profiles on Piston Ring Radial Dynamics," ASME J. Eng. Gas Turbines Power, **125**, pp. 1081–1089.
[33] Haywood, J. B., 2003, "An Improved Friction Model for Spark-Ignition Engines," SAE Paper No. 2003-01-0725.
[34] Livanos, G., and Kyrtatos, N. P., 2006, "A Model of the Friction Losses in Diesel Engines," SAE Paper No. 2006-01-0888.
[35] Taylor, R., 1997, "Engine Friction: The Influence of Lubricant Rheology," Proc. Inst. Mech. Eng., Part J: J. Eng. Tribol., **211**(3), pp. 235–246.
[36] Allen, D. G., Dudely, B. R., Middletown, J., and Panka, D. A., 1976, "Prediction of Piston Ring Cylinder Bore Oil Film Thickness in Two Particular Engines and Correlation With Experimental Evidences," *Piston Ring Scuffing*, Mechanical Engineering Publication Ltd., London, p. 107.

[37] Harigaya, Y., Akagi, J., and Suzuki, M., 2000, "Prediction of Temperature Viscosity and Thickness in Oil Film Between Ring and Liner of Internal Combustion Engines," *CEC and SAE Spring Fuels and Lubricants Meeting*, Paris, France, Jun. 2000, Paper No. 200011790.

[38] Harigaya, Y., Suzuki, M., and Takiguchi, M., 2003, "Analysis of Oil Film Thickness on a Piston Ring of Diesel Engine: Effect of Oil Film Temperature," ASME J. Eng. Gas Turbines Power, **125**, pp. 596–603.

[39] Harigaya, Y., Suzuki, M., Toda, F., and Takiguchi, M., 2006, "Analysis of Oil Film Thickness and Heat Transfer on a Piston Ring of a Diesel Engine: Effect of Lubricant Viscosity," ASME J. Eng. Gas Turbines Power, **128**, pp. 685–693.

[40] Takiguchi, M., Sasaki, R., Takahashi, I., Ishibashi, F., Furuhama, F., Kai, R., and Sato, M., 2000, "Oil Film Measurement and Analysis of a Three Ring Pack in an Operating Diesel Engine," *CEC and SAE Spring Fuels and Lubricants Meeting*, Paris, France, Jun. 2000, Paper No. 200011787.

[41] Tamminen, J., Sanddtröm, C., and Andersson, P., 2006, "Influence of Load on the Triboligical Conditions in Piston Ring and Cylinder Liner Contacts in a Medium-Speed Diesel Engine," Tribol. Int., **39**, pp. 1643–1652.

[42] Sonntag, R., Borgnakke, C., and Van Wylen, G., 1998, *Fundamentals of Thermodynamics*, 5th ed., Wiley, New York.

[43] Burcat, A., and Ruscic, B., 2005, "Third Millennium Ideal Gas and Condensed Phase Thermochemical Database for Combustion With Updates from Active Thermochemical Tables," Argonne National Laboratory Report No. ANL-05/20, http://www.chem.leeds.ac.uk/combustion/combustion.html.

[44] Woschni, G., 1967, "Universally Applicable Equation for the Instantaneous Heat Transfer Coefficient in Internal Combustion Engine," SAE Paper No. 670931.

[45] Karamangil, M., Kaynakli, O., and Surmen, A., 2006, "Parametric Investigation of Cylinder and Jacket Side Convective Heat Transfer Coefficients of Gasoline Engines," Energy Convers. Manage., **47**, pp. 800–816.

[46] Stone, R., 1999, *Introduction to Internal Combustion Engines*, 3rd ed., Palgrave, New York.

[47] Branes-Moss, H. W., 1975, "A Designer's Viewpoint in Passenger Car Engines," *Conference Proceedings*, Institution of Mechanical Engineers, London, pp. 133–145.